

SEMI-ORTHOGONAL FUNCTIONS FOR THE INTERNAL APPROXIMATION OF NULL-CONTROLS AND A HEAT SOURCE INVERSE PROBLEM

Axel Osses, Felipe Urrutia

▶ **To cite this version:**

Axel Osses, Felipe Urrutia. SEMI-ORTHOGONAL FUNCTIONS FOR THE INTERNAL APPROXIMATION OF NULL-CONTROLS AND A HEAT SOURCE INVERSE PROBLEM. 2023. hal-04297658v1

HAL Id: hal-04297658

https://hal.science/hal-04297658v1

Preprint submitted on 21 Nov 2023 (v1), last revised 23 Nov 2023 (v2)

HAL is a multi-disciplinary open access archive for the deposit and dissemination of scientific research documents, whether they are published or not. The documents may come from teaching and research institutions in France or abroad, or from public or private research centers.

L'archive ouverte pluridisciplinaire **HAL**, est destinée au dépôt et à la diffusion de documents scientifiques de niveau recherche, publiés ou non, émanant des établissements d'enseignement et de recherche français ou étrangers, des laboratoires publics ou privés.



Distributed under a Creative Commons CC BY-NC-SA 4.0 - Attribution - Non-commercial use - ShareAlike - International License

SEMI-ORTHOGONAL FUNCTIONS FOR THE INTERNAL APPROXIMATION OF NULL-CONTROLS AND A HEAT SOURCE INVERSE PROBLEM

FELIPE URRUTIA[(1)] AND AXEL OSSES[(1,2)]

Abstract. We optimized the construction and computation of null controls for the heat equation using a suitable basis, which we call the semi-orthogonal functions for internal approximation or SOFIA basis. These functions are locally orthogonal to the standard spectral basis of the corresponding elliptic operator in the observation region. We then consider the application of these null controls to the inverse problem of recovering the spatial part $f(x)$ of a source term $f(x)\sigma(t)$ with separated variables in the heat equation from internal observations of the solution and its time derivative in an observatory $\mathcal{O}$. By incorporating the SOFIA basis to a duality method that uses a family of null controls to compute the Fourier coefficients of the source $f(x)$, we achieve noise robustness, good accuracy and numerical efficiency.

1. Introduction

Given a final time $T > 0$ and a regular and bounded domain Ω in $\mathbb{R}^n$ with boundary $\partial\Omega$, we consider the heat equation:

$$\begin{cases} \partial_t u(x,t) - \operatorname{div}(\gamma \nabla u(x,t)) = f(x)\sigma(t), & \text{in } \Omega \times (0,T), \\ u(x,t) = 0, & \text{on } \partial\Omega \times (0,T), \\ u(x,0) = 0, & \text{in } \Omega, \end{cases} \tag{1}$$

where $\gamma \in L^\infty(\Omega)$ with $\gamma \geq \gamma_0 > 0$ a.e. in Ω is the heat conductivity (that we assume independent of time). The term $f(x)\sigma(t)$ represents a source term with separated variables with $\sigma \in W^{1,\infty}(\Omega)$ and $f \in L^2(\Omega)$. The inverse problem consists in recovering f, assuming that σ is known, from observations of the solution u and its time derivative u_t in an open and non empty observatory $\mathcal{O} \subset \Omega$ and during a time interval $(0,T)$, $T > 0$.

The problem of identifying the spatial part of the source for the heat equation, which is closely linked to the problem of recovering the initial condition for the heat equation, is a severely ill posed problem. In fact, it is well known that this problem has logarithmic stability even if f has some extra regularity than the original L^2 regularity, see for instance [12].

[(1)] Center for Mathematical Modeling, FCFM, Universidad de Chile, IRL CNRS 2807

[(2)] Departamento de Ingeniería Matemática, FCFM, Universidad de Chile

E-mail addresses: furrutia@dim.uchile.cl, axosses@dim.uchile.cl.

This is one of the reasons why this problem has attracted a large interest in the control and inverse problem communities for decades. Let us mention a non exhaustive list of some previous studies to give an idea of similar or complementary inverse source problems related to the one of this paper: i) the recovery of sources of the form $f = \chi_D$, where χ_D is the indicatrix function of an unknown subset D of Ω, see for instance [15] where domain derivative techniques are used, ii) the identification of point sources of type $f = \sum_{j=1}^{N} p_j \delta_{x_j,t_j}$ with weights p_j and located at some points $(x_j, t_j) \in \Omega \times (0, T)$ as in [21], [31] or [8], where the backwards heat equation is used, iii) the determination of when and where the source appears in the equation, that is, to know x_0 and T_0 such that $f(x_0, T_0) \neq 0$ for the first time, as was studied in [17] where indicatrix functionals are introduced, iv) the reconstruction of initial temperature backward heat equation, see for instance [20] and the references therein and v) the structural identification of sources of the form $f(x)R(x,t)$ where R is known, as appears when using the Buckheim-Klibanov approaches and Global Carleman iniqualities or more generally of the form $f(x,u)R(x,t)$ in nonlinear equations [2], [1] or [5], [4].

Among the applications of these types of inverse source problems, let us mention the following: a) the identification of pollutant, radioactive, or odor emissions in atmospheric chemistry on a global, regional, or city scale [6], [29], [14], b) the identification of water pollution in coastal areas, lakes, rivers, [7], [25], c) the optimal design of monitoring networks [28], [14], d) the detection and attribution of climate change [27], [11], e) the detection of phase transition (coupled heat equations) [16], f) the identification of three dimensional images in laser microscopy which is related to some backwards heat equation [26], etc.

Let us now return to the inverse problem. This was previously considered in [10] where the key finding was a reconstruction formula for $f(x)$ (see Theorem 8 later). This formula was obtained by extending a duality method originally proposed in [30] for hyperbolic equations. A common feature of these methods is that they both use exact null-controls. In the hyperbolic case of [30], a single null-control is needed, whereas in the parabolic case of [10], a continuous family of exact controls is required. Nevertheless, the main drawback of the proposed algorithm in [10] is that the calculation of the family of null controls is computationally expensive and inaccurate.

Our main result is the introduction of a special basis that we will call the SOFIA basis, which allows us to easily compute null-controls and identify sources for the heat-equation using the method introduced in [10]. The existence of the SOFIA basis is equivalent to the Lebeau–Jerison property of the quantitative unique continuation for finite linear combinations of eigen-frequencies for an elliptic operator [19]. Therefore, the method can be easily extended to similar null-control and source inverse problem for the Stokes equation as we did in [13] for example, using the corresponding quantitative unique continuation for finite linear combinations of eigen-frequencies for the Stokes operator[3]. The method of null controls based on the SOFIA basis we present here can be also extended to hyperbolic equations as it was originally published by [30].

The explicit computation of null-controls for the heat equation using the SOFIA basis let us to have a more explicit reconstruction formula for the Fourier coefficients of the source term $f(x)$ with respect to that have been previously done in [10] and to obtain significantly better numerical accuracy and shorter running. In particular, the proposed method of this article does not need to solve optimization problems for computing the null-controls nor to solve Volterra equations for the source term, and these facts dramatically diminish the computer time and improve accuracy. This also renders the source recovery method originally proposed by [10] more attractive and useful for practical applications. At the same time, the proposed method allow for efficiently compute null controls for parabolic equations in general (see Figure 3), problem that has strong interest by itself. Indeed, there has been important effort to develop efficient and accurate numerical algorithms and/or analytical approximations to compute null controls for parabolic equations and systems in practice [22], [23], [24]

The rest of the article is organized as follows. In Section 2 we present the SOFIA basis and the application to the computation of null-controls for the heat equation. In Section 3 we give the application of the SOFIA basis to the reconstruction of sources for the heat equation and in Section 4 we show some numerical experiments that shows the practical performance of the method.

2. SOFIA basis and null controllability results

Let Ω be a non-empty and open domain subset of $\mathbb{R}^n$ with a smooth boundary $\partial\Omega$, and let $\mathcal{O} \subseteq \Omega$ be an observatory region where the measurements of the solution will be available. Since we will link by duality the observation region for the inverse problem with the support of the controls, we will consider first the null controllability problem for the heat equation for a given final time $\tau \in (0, T]$, as follows:

$$\begin{cases} u_t - \operatorname{div}(\gamma \nabla u) = v^{(\tau)} \mathbf{1}_{\mathcal{O}}, & \text{in } \Omega \times (0,\tau), \\ u(x,t) = 0, & \text{on } \partial\Omega \times (0,\tau), \\ u(x,0) = u_0(x), & \text{in } \Omega, \end{cases} \tag{2}$$

with $u_0 \in L^2(\Omega)$. The problem of internal null controllability in time $\tau > 0$ consists in finding a control $v^{(\tau)} \in L^2(\mathcal{O} \times (0,\tau))$ applied in the indicatrix $\mathbf{1}_{\mathcal{O}}$ of the observatory, such that the solution u of the controlled heat equation (2) satisfies the final condition:

$$u(x,\tau) = 0 \quad \text{a.e. in } \Omega. \tag{3}$$

The existence of internal null controls can be directly obtained using global Carleman inequalities [9].

In this work we investigate how to approximate null controls for the heat equation using the spectral decomposition of the solution u by the eigenfunctions of the Laplace operator in combination with a family of functions that we will call the Semi-Orthogonal Functions for the Internal Approximation (SOFIA). Figure 1 gives a first graphical idea of the functions of the SOFIA basis that are supported into the observation/control region $\mathcal{O}$.

We introduce the eigen-values and eigen-functions $\{(\lambda_k, \varphi_k)\}_{k\geq 1}$ of the underlying elliptic operator associated to problem (1) as follows:

$$\begin{cases} -\operatorname{div}(\gamma \nabla \varphi_k) = \lambda_k \varphi_k, & \text{in } \Omega, \\ \varphi_k = 0, & \text{on } \partial\Omega, \end{cases} \tag{4}$$

where $\varphi_k \in H_0^1(\Omega)$ form an orthonormal basis in $L^2(\Omega)$ with an non decreasing sequence

$$0 < \lambda_1 \leq \lambda_2 \leq \ldots \leq \lambda_k \leq \ldots$$

From the practical point of view, we will consider for the approximation of the null controls only a finite number of eigen-functions, say $(\varphi_k)_{k=1,\ldots,K}$, where K is the number of the first selected eigen-functions.

Definition 1. *Given the first K (orthonormal) eigen-functions $(\varphi_k)_{k=1,\ldots,K}$ of (4) and a open and nonempty observatory $\mathcal{O} \subset \Omega$, we define the first K semi-orthogonal functions for internal approximation (that we call the SOFIA family) $(\psi_p)_{p=1,\ldots,K}$ by the equations:*

$$\langle \varphi_k, \psi_p \rangle_{L^2(\mathcal{O})} = \delta_{k,p}, \quad 1 \leq k, p \leq K, \tag{5}$$

and extended by zero outside $\mathcal{O}$.

The following result states that the SOFIA family is well defined.

Lemma 2. *The SOFIA family in the observatory $\mathcal{O}$ defined by (5) always exists for any $K \geq 1$ and can be computed from a linear system with a $K \times K$ positive definite matrix $A_K = (A_K)_{k,k'} = (\varphi_k, \varphi_{k'})_{L^2(\mathcal{O})}$ such that there exist two constants C_1 and C_2 such that*

$$A_K \xi \cdot \xi \geq C_1 e^{-C_2\sqrt{K}}, \quad \forall \xi \in \mathbb{R}^n.$$

Moreover, there exists a sequence $\widehat{\xi}_K$ in $\mathbb{R}^n$ with $|\widehat{\xi}_K| = 1$ and constants C_3 and C_4 such that

$$A_K \widehat{\xi}_K \cdot \widehat{\xi}_K = C_3 e^{-C_4\sqrt{K}} \to 0, \quad \text{as } K \to \infty.$$

Remark 3. *Notice that the matrix A_K is the same for the computation of the whole SOFIA basis $(\psi_p)_{p=1,\dots,K}$ and when $K \to \infty$ the matrix A become singular. See the behaviour of the condition number of the matrix A_K as a function of K in an example in Figure 2.*

Proof. Given p with $1 \leq p \leq K$, we can reduce the problem (5) of finding each function ψ_p to a linear problem. For doing this, we consider a solution of the form $\psi_p = \sum_{k'=1}^{K} \alpha_{k'}^{(p)} \varphi_{k'}$. Therefore, for each $1 \leq k \leq K$ if we multiply ψ_p by φ_k and we integrate in $\mathcal{O}$, by using the orthogonality condition (5) we obtain:

$$\sum_{k'} \alpha_{k'}^{(p)} \langle \varphi_k, \varphi_{k'} \rangle_{L^2(\mathcal{O})} = \delta_{p,k}. \tag{6}$$

If we define the $K \times K$ matrix $A_K = (\langle \varphi_k, \varphi_{k'} \rangle_{L^2(\mathcal{O})} : 1 \leq k, k' \leq K)$ then $\alpha^{(p)}$ will be the unique solution of the linear system $A_K \alpha^{(p)} = e_p$, where e_p is the p-th vector of the canonical basis. Therefore, it suffices to prove that A_K is a non-singular matrix and moreover a positive definite matrix. Indeed

$$A_K \xi \cdot \xi = \sum_{k=1}^{K} \sum_{k'=1}^{K} \langle \varphi_k, \varphi_{k'} \rangle_{L^2(\mathcal{O})} \xi_k \xi_{k'} = \left\langle \sum_{k=1}^{K} \varphi_k \xi_k, \sum_{k'=1}^{K} \varphi_{k'} \xi_{k'} \right\rangle_{L^2(\mathcal{O})}.$$

If we define $v = \sum_{k'=1}^{K} \varphi_{k'} \xi_{k'}$, since v is a linear combination of eigen-functions of an elliptic operator, therefore by quantified unique continuation [19] we have that there exist positive constants C_1 and C_2 such that

$$A_K \xi \cdot \xi = ||v||^2_{L^2(\mathcal{O})} \geq C_1 e^{-C_2\sqrt{K}} ||v||^2_{L^2(\Omega)} = C_1 e^{-C_2\sqrt{K}} |\xi|^2.$$

On the other hand we know from [19] that the above estimate is optimal, i.e., for each K there exist a vector ξ_K (that contains the coefficients of the "worst case" linear combination of the eigen-functions) and positive constants C_3 and C_4 such that for $v_K = \sum_{k'=1}^{K} \varphi_{k'} \xi_{K,k'}$ we have

$$A_K \xi_K \cdot \xi_K = ||v_K||^2_{L^2(\mathcal{O})} = C_3 e^{-C_4\sqrt{K}} ||v_K||^2_{L^2(\Omega)} = C_3 e^{-C_4\sqrt{K}} |\xi_K|^2$$

and we obtain the result after normalizing $\widehat{\xi}_K = \xi_K / |\xi_K|$. □

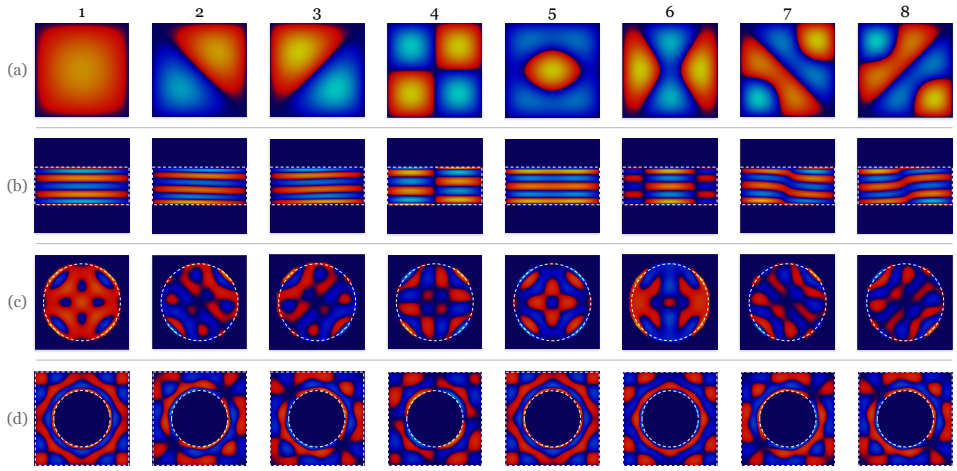


FIGURE 1. The first eight eigen-functions of the Laplace operator in a square domain (upper row) together with their associated semi-orthogonal functions for the internal approximation (SOFIA) (last three rows) for a rectangular, circular and complement of an circular observation/control region. (**a**) Classical eigen-functions in the whole domain, (**b**) SOFIA in a rectangular observation region, (**c**) in a circular observation region, and (**d**) in the complement of an circular observation region.

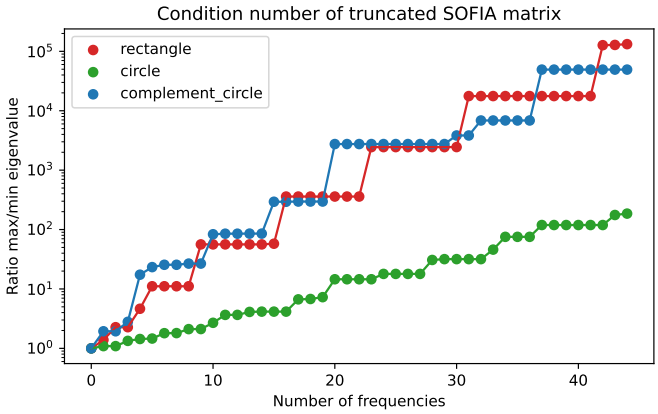


FIGURE 2. Condition number of the matrix A_K, with $K = 1, ..., 45$, for rectangular, circular and complement of an circular observation/control region.

The introduction of SOFIA family serves to approximately compute null controls for the heat equation. In fact, we have the following result.

Definition 4. *We say that $v^{(\tau,K)}$ is an approximate internal null control for (2) if, given an approximate solution of problem (2) in $\Omega \times (0,\tau)$ of the form*

$$u^K(x,t) = \sum_{k=1}^{K} \alpha_k(t)\varphi_k(x),$$

it satisfies $u^K(\tau,x) = 0$ a.e. in Ω.

Theorem 5. *Let $\{\psi_k\}_{k=1}^K$ be the SOFIA basis. For all $\rho \in L^1(0,\tau)$ such that*

$$\int_0^\tau e^{\lambda_k s}\rho(s)ds \neq 0, \qquad \forall k = 1,\dots,K \tag{7}$$

then

$$v^{(\tau,K)}(x,t) = \sum_{k=1}^{K} c_k(\tau;\rho)\psi_k(x)\rho(t) \tag{8}$$

with

$$c_k(\tau;\rho) = -\frac{\langle u_0,\varphi_k\rangle_{L^2(\Omega)}}{\int_0^\tau e^{\lambda_k s}\rho(s)ds}, \quad k = 1\dots,K, \tag{9}$$

is an approximate internal null control for problem (2).

Remark 6. *Find functions ρ such that (7) holds is not difficult, for instance, take $\rho = \rho_0$ a non zero constant, in which case $c_k = -\frac{\lambda_k\langle u_0,\varphi_k\rangle_{L^2(\Omega)}}{\rho_0(e^{\lambda_k\tau}-1)}$, or more generally, if ρ has constant sign a.e. in $[0,\tau]$. See Figure 3 to see the behavior of the approximate null-controls for different choices of ρ.*

Remark 7. *One interesting choice to have (7) is taking $\rho(t) = e^{\beta t} - 1$ with $\beta > 0$ that works from the previous remark, or $\beta = \lambda_k$ in whose case the coefficients are explicitly given by $c_k = -\frac{2\lambda_k\langle u_0,\varphi_k\rangle_{L^2(\Omega)}}{1+(e^{\lambda_k\tau}-1)^2}$. Conversely, if $\beta = -\lambda_k$, it is not difficult to see that (7) does not hold for a sequence $\tau_k = \frac{e^{\lambda_k\tau}-1}{\lambda_k}$.*

Proof. By replacing

$$u^K(t,x) = \sum_{k=1}^{K} \alpha_k(t)\varphi_k(x) \tag{10}$$

in equation (2) and using the L^2-orthogonality of the eigen-functions and the SOFIA basis property (5) we obtain that α_k satisfies

$$\begin{cases} \alpha_k' + \lambda_k\alpha_k = \int_{\mathcal{O}} v^{(\tau)}(x,t)\varphi_k(x) = c_k(\tau;\rho)\rho(t), & \text{in } (0,\tau), \\ \alpha_k(0) = \langle u_0,\varphi_k\rangle_{L^2(\Omega)} \end{cases} \tag{11}$$

with explicit solution given by

$$\alpha_k(t) = e^{-\lambda_k t}\left(\langle u_0,\varphi_k\rangle_{L^2(\Omega)} + c_k(\tau;\rho)\int_0^t e^{\lambda_k s}\rho(s)ds\right) \tag{12}$$

and after imposing $u^K(t,\tau) = 0$, i.e. $\alpha_k(\tau) = 0$ for all $k = 1, \dots, K$, we obtain

$$c_k(\tau;\rho) = \frac{-\langle u_0, \varphi_k \rangle_{L^2(\Omega)}}{\int_0^\tau e^{\lambda_k s}\rho(s)ds}, \quad k = 1, \dots, K. \tag{13}$$

□

The behavior of some of these null-controls are depicted in Figure 3 for three different functions ρ and compared with the classical L^2-optimal control that minimize $\|u(\tau,\cdot)\|_{L^2(\Omega)}$.

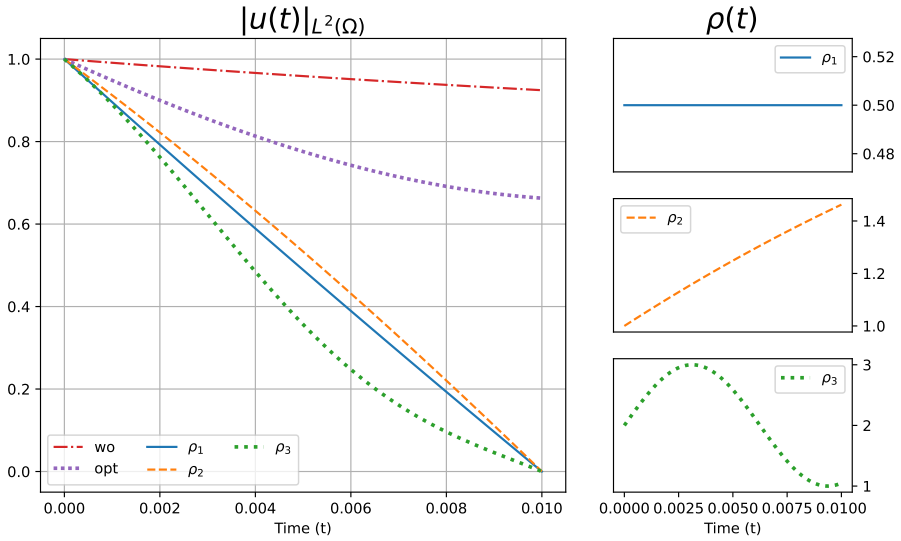


FIGURE 3. Norm of the controlled solution ($\gamma = 1$) with initial condition $u_0 = \varphi_1$ in the domain $\Omega = (0,1)^2$ and in the interval $(0,\tau]$, $\tau = 0.01$ for different approximate internal null-controls given by (8) in a region $\mathcal{O} = \{1/3 < y < 2/3\}$ for different choices of ρ: (wo) uncontrolled solution, (opt) L^2-optimal control, (ρ_1) constant, (ρ_2) increasing of the form $1 + 0.075t - 0.0014t^2$ and (ρ_3) oscillating of the form $2 + \sin(0.314t)$.

We show now how to use the SOFIA basis can be used to solve the heat source inverse problem.

3. SOFIA BASIS AND SOURCE RECONSTRUCTION FORMULAS

Let τ be an intermediate time in $(0,T]$, and let φ_k be an eigen-function in $L^2(\Omega)$ of (4). We know that [9, 18] there exists a control $v_k^{(\tau)} \in L^2(\mathcal{O}\times(0,\tau))$

such that the solution ϕ of the problem

$$\begin{cases} -\phi_t - \operatorname{div}(\gamma\nabla\phi) = v_k^{(\tau)}\mathbf{1}_{\mathcal{O}}, & \text{in } \Omega\times(0,\tau),\\ \phi(x,t) = 0, & \text{on } \partial\Omega\times(0,\tau),\\ \phi(x,\tau) = \varphi_k, & \text{in } \Omega, \end{cases} \tag{14}$$

satisfies

$$\phi(x,0) = 0, \quad \text{a.e. in } \Omega. \tag{15}$$

While in [10] we computed null controls by minimizing a sequence of optimal control problems, in our work, we will use the SOFIA basis. For this we introduce the Volterra operator.

For $\sigma \in C^1([0,\tau])$ and $\tau \in (0,T]$, we will denote by $V^{(\tau)}$ the Volterra operator given by

$$\left(V^{(\tau)}\theta\right)(t) = \sigma(0)\theta'(t) + \int_t^\tau (\sigma(s-t)\theta(s) + \sigma'(s-t)\theta'(s))ds \tag{16}$$

where θ is any function in $C^1([0,\tau])$ such that $\theta(\tau) = 0$. It is worth noting that $V^{(\tau)}$ is a linear operator.

Let $f \in L^2(\Omega)$ be the unknown source in (1) with the known time dependency $\sigma \in C^1([0,T])$ and $\sigma(T) \neq 0$. According to Theorem 1.6 in [10], we have the following result:

Theorem 8 ([10])**.** *The Fourier coefficients $f_k = \langle f, \varphi_k\rangle_{L^2(\Omega)}$ of the source f are given by the formula*

$$f_k = a_k^{-1}(C_k^1 + C_k^2), \tag{17}$$

provided that σ is such that the coefficients a_k defined by

$$a_k = 1 - \frac{\lambda_k}{\sigma(T)}\int_0^T e^{-\lambda_k(T-s)}\sigma(s)ds \tag{18}$$

does not vanish. Furthermore, C_k^1 and C_k^2 are given by

$$C_k^1 = -\tfrac{\sigma(0)}{\sigma(T)}\langle u, \theta_k^{(T)}\rangle_{H^1(0,T;L^2(\mathcal{O}))}, \tag{19}$$

$$C_k^2 = -\tfrac{1}{\sigma(T)}\int_0^T \sigma'(T-\tau)\langle u, \theta_k^{(\tau)}\rangle_{H^1(0,T;L^2(\mathcal{O}))}d\tau, \tag{20}$$

where $\theta_k^{(\tau)}$ is the solution to the Volterra equation, i.e.

$$V^{(\tau)}\theta_k^{(\tau)} = v_k^{(\tau)} \tag{21}$$

and the $H^1(0,\tau;L^2(\mathcal{O}))$ product is given by

$$\langle u, \theta_k^{(\tau)}\rangle_{H^1(0,\tau;L^2(\mathcal{O}))} = \int_0^\tau \left(\langle u, \theta_k^{(\tau)}\rangle_{L^2(\mathcal{O})} + \langle u_t, \partial_t\theta_k^{(\tau)}\rangle_{L^2(\mathcal{O})}\right)dt. \tag{22}$$

Proof. In order to be self-contained, we give here a brief proof of the result following [10]. If w is the solution of $w_t - \operatorname{div}(\gamma\nabla w) = 0$ in $\Omega\times(0,T)$ with $w(0) = f(x)$ in Ω and $w = 0$ on the boundary, then for each x, the convolution operator $u(x,\cdot) = \sigma * w(x,\cdot) = Kw$ which is in fact the dual

operator in $H^1(0,\tau)$ of $V^{(\tau)}$ defined in (16), satisfies the problem (1). By differentiating u with respect to time and after evaluating in $t=T$:

$$\sigma(0)w(T)+\int_0^T \sigma'(T-\tau)w(\tau)d\tau = \operatorname{div}(\gamma\nabla u(T))+\sigma(T)f(x).$$

Multiplying the previous expression by φ_k and integrating over Ω gives

$$\sigma(T)f_k = -\int_\Omega \operatorname{div}(\gamma\nabla u(T))\varphi_k + \sigma(0)\int_\Omega w(T)\varphi_k + \int_0^T \sigma'(T-\tau)\int_\Omega w(\tau)\varphi_k\, d\tau.$$

From the definition of null controls v^τ given by (14)-(15) and extended by zero in $[\tau,T]$, after integrating by parts, we have that for all $\tau\in(0,T]$

$$\int_0^\tau\int_{\mathcal{O}} wv^{(\tau)} = \int_0^\tau\int_\Omega w(-\phi_t-\operatorname{div}(\gamma\nabla\phi))dt = -\int_0^\tau w(\tau)\varphi_k.$$

Therefore using the definition of $\theta_k^{(\tau)}$ of (21), also extended by zero in $[\tau,T]$, we obtain

$$\begin{aligned}\sigma(T)f_k &= -\int_\Omega \operatorname{div}(\gamma\nabla u(T))\varphi_k - \sigma(0)\underbrace{\int_0^T\int_{\mathcal{O}} wv^{(T)}}_{(w,V^{(T)}\theta^{(T)})}\\ &\quad -\int_0^T\sigma'(T-\tau)\underbrace{\int_0^T\int_{\mathcal{O}} wv^{(\tau)}}_{(w,V^{(\tau)}\theta^{(\tau)})}d\tau\end{aligned}$$

and by duality

$$\begin{aligned}\sigma(T)f_k &= \lambda_k\int_\Omega u(T)\varphi_k - \sigma(0)(u,\theta^T)_{H^1(0,T,L^2(\mathcal{O}))}\\ &\quad -\int_0^T\sigma(T-\tau)(u,\theta^\tau)_{H^1(0,\tau),L^2(\mathcal{O})}.\end{aligned}$$

Now using that $u(T)=\int_0^T e^{-\lambda_k(T-s)}f(x)\sigma(s)ds$ we have

$$\begin{aligned}\sigma(T)f_k &= \lambda_k f_k\int_0^T e^{-\lambda_k(T-s)}\sigma(s)ds - \sigma(0)(u,\theta^T)_{H^1(0,T,L^2(\mathcal{O}))}\\ &\quad -\int_0^T\sigma(T-\tau)(u,\theta^\tau)_{H^1(0,\tau),L^2(\mathcal{O})}\end{aligned}$$

that is

$$\begin{aligned}\sigma(T)f_k\left(1-\lambda_k\int_0^T e^{-\lambda_k(T-s)}\sigma(s)ds\right) &= -\sigma(0)(u,\theta^T)_{H^1(0,T,L^2(\mathcal{O}))}\\ &\quad -\int_0^T\sigma(T-\tau)(u,\theta^\tau)_{H^1(0,\tau),L^2(\mathcal{O})}.\end{aligned}$$

Finally, by defining (18) we obtain the coefficients (19) of the formula. □

In [10], the coefficients C_k^1 and C_k^2 are recovered from numerical approximations of $\theta_k^{(\tau)}$, the solutions of the Volterra equation for any $k-$th frequency and a discrete set of intermediate times τ in $(0,T]$. However, we can explicitly find the coefficients here.

Indeed, using the SOFIA basis, we have the following representation formula for recovering the source term in the heat equation.

Theorem 9. *If $\sigma \in C^1([0,T])$ with $\sigma(T) \neq 0$ and $\{\psi_k\}_{k=1}^K$ is the SOFIA basis, then the Fourier coefficients of the source term f in (1) are given by $f_k = a_k^{-1}(C_k^1+C_k^2)$, $k=1,\dots,K$, provided that $a_k = 1-\frac{\lambda_k}{\sigma(T)}\int_0^T e^{-\lambda_k(T-s)}\sigma(s)ds \neq 0$ where*

$$C_k^1 = -\overline{c}_k(T;V^{(T)}\rho_T)\frac{\sigma(0)}{\sigma(T)}\int_0^T \langle \rho_T u + \rho_T' u_t, \psi_k\rangle_{L^2(\mathcal{O})}dt, \tag{23}$$

$$C_k^2 = -\overline{c}_k(\tau;V^{(\tau)}\rho_\tau)\frac{1}{\sigma(T)}\int_0^\tau \langle \rho_\tau u + \rho_\tau' u_t, \psi_k\rangle_{L^2(\mathcal{O})}dt \tag{24}$$

where $\overline{c}_k$ are given by (27) for any $\rho_\tau \in C^1([0,\tau])$, $\tau \in (0,T]$ such that $\rho_\tau(\tau)=0$ and satisfying

$$(e^{\lambda_k t} * V^{(\tau)}\rho_\tau)(\tau) \neq 0 \tag{25}$$

for all $k=1,\dots,K$.

Proof. Indeed, if for any $\rho_\tau \in C^1([0,\tau])$ with $\rho_\tau(\tau)=0$ we define

$$\theta_k^{(\tau)}(x,t) = \overline{c}_k(\tau;V^{(\tau)}\rho_\tau)\psi_k(x)\rho_\tau(t) \tag{26}$$

where

$$\overline{c}_k(\tau;\rho_\tau) = -\frac{1}{\int_0^\tau e^{\lambda_k s}(V^{(\tau)}\rho_\tau)(\tau-s)ds} = -\frac{1}{(e^{\lambda_k t} * V^{(\tau)}\rho_\tau)(\tau)}, \tag{27}$$

then

$$v_k^{(\tau)}(x,t) = (V^{(\tau)}\theta_k^{(\tau)}(x,\cdot))(t) = \overline{c}_k(\tau,V^{(\tau)}\rho_\tau)\psi_k(x)(V^{(\tau)}\rho_\tau)(t) \tag{28}$$

is an internal null-control for (14) thanks to Theorem 5 and therefore

$$\langle u, \theta_k^{(\tau)}\rangle_{H^1(0,\tau;L^2(\mathcal{O}))} = \overline{c}_k(\tau;V^{(\tau)}\rho_\tau)U_k(\tau;\rho_\tau) \tag{29}$$

where

$$U_k(\tau;\rho) = \int_0^\tau \left(\rho_\tau(t)\langle u(\cdot,t),\psi_k\rangle_{L^2(\mathcal{O})} + \rho_\tau'(t)\langle u_t(\cdot,t),\psi_k\rangle_{L^2(\mathcal{O})}\right)dt \tag{30}$$

and after replacing this in the coefficients C_k^1 and C_k^2 of Theorem 8 we finish the proof. □

Remark 10. *Notice that it is not necessary to compute null-controls nor to solve any Volterra equation using the above representation. The only computation is the calculation of the SOFIA basis $\{\psi_k\}_k$ and the corresponding integrals with the measurements of u and u_t in the observatory $\mathcal{O}$.*

Remark 11. *Note that the implementation of the algorithm presented in the previous theorem can be done sequentially. Indeed, once you have computed an approximation of the source from measurements of the solution in* $\mathcal{O} \times [0,T]$*, as new measurements are available in* $\mathcal{O}\times[T,T+\Delta t]$ *for some* $\Delta T > 0$*, we can update the coefficients by adding the corresponding integrals between* T *and* $T+\Delta t$*, without recalculating the SOFIA basis which is independent of time.*

Remark 12. *In* [10] *we have studied cases when* σ *satisfies that the coefficients* a_k *do not vanish, they include i)* σ *constant, ii)* σ *strictly increasing or decreasing and iii)* σ *of type* $\sin(\omega t)$ *except for a discrete number of frequencies* ω*.*

Unfortunately, we do not have an explicit class of functions ρ_τ (possibly depending on k) such that the coefficients $\bar{c}_k$ of Theorem 9 are well defined, i.e. such that condition (25) is satisfied. Nevertheless, we have the following characterization that can help to check this condition in practice.

Lemma 13. *For every* $\rho_\tau \in C^1([0,\tau])$ *we have*

$$(e^{\lambda_k t} * V^{(\tau)}\rho_\tau)(\tau) = \langle \sigma * e^{\lambda_k(\tau-\cdot)}, \rho_\tau \rangle_{H^1(0,\tau)}. \tag{31}$$

Proof. The proof is by duality as in [10]. Let us define $h(s) = e^{\lambda_k(\tau-s)}$ then

$$\begin{gathered}(e^{\lambda_k t} * V^{(\tau)}\rho_\tau)(\tau) = \int_0^\tau h(s)(V^{(\tau)}\rho_\tau)(s)ds \\ = \int_0^\tau \sigma(0)\rho_\tau'(s)h(s)ds + \\ \int_0^\tau \int_s^\tau (\sigma'(t-s)\rho_\tau'(t)h(s) + \sigma(t-s)\rho_\tau(t)h(s))\, dtds \\ = \int_0^\tau \int_0^t \sigma(t-s)h(s)\rho_\tau(t)dsdt + \int_0^\tau \partial_t \left[\int_0^t \sigma(t-s)h(s)ds\right] \rho_\tau'(t)dt.\end{gathered}$$

□

Remark 14. *The previous lemma suggests to choose* $\rho_\tau = \sigma * e^{\lambda_k(\tau-\cdot)}$ *since that makes the* H^1 *product positive, but this does not necessarily fulfill the hypothesis* $\rho_\tau(\tau) = 0$ *of Theorem 9. The optimal choice of* ρ_τ *is an open problem and we think it out of the scope of the present paper and so it would be the subject of a forthcoming study.*

4. Numerical simulations

We fix $\Omega = (0,1)^2$ and $T = 0.1$. For the numerical integrations in time we choose a time step $\Delta t = \Delta\tau = 10^{-3}$. We use a constant diffusion $\gamma = 1/5$ for all the examples. We consider three different observation sets. The first one is the rectangle $\mathcal{O} = (0,1)\times(0.3,0.7)$, the second one is the circle $\mathcal{O} = B((0.5,0.5),0.42)$ and the third one is the complement of an circle $\mathcal{O} = \Omega \setminus B((0.5,0.5),0.94)$. We select for all our tests the first $K = 45$ eigenvalues and eigenfunctions $(\lambda_k,\varphi_k)_{k\geq 1}$. We use the SLEPc method from FeniCs to solve the eigenvalue problem and to compute the SOFIA matrix with finite elements with a continuous Galerkin space of type Lagrange with degree 3, mesh size $h = 1/64$. In order to solve the SOFIA linear system, we

use the GESV method from SciPy python library. We set $\rho_{\tau,\beta}(t) = e^{\beta t} - e^{\beta\tau}$, $t \in (0, \tau]$ (notice that $\rho_{\tau,\beta}(\tau) = 0$) with a fixed $\beta > 0$ for any τ, where the value of β is such that condition (25) is verified on each experiment.

Following [10], we consider three different time dependencies of the source (see Figure 4):

(a) $\sigma_0 = 1$,
(b) $\sigma_1 = 1 + 2t/t_0 - (t/t_0)^2$ if $t < t_0$, else 2, with $t_0 = 3/40$,
(c) $\sigma_2 = 2 + \sin\left(4\frac{\pi t}{T-\epsilon}\right)$ if $t < T - \epsilon$, else $3/2$, with $\epsilon = 10^{-5}$.

Notioce that all tested σ functions exhibit positivity within the interval $(0, T]$.

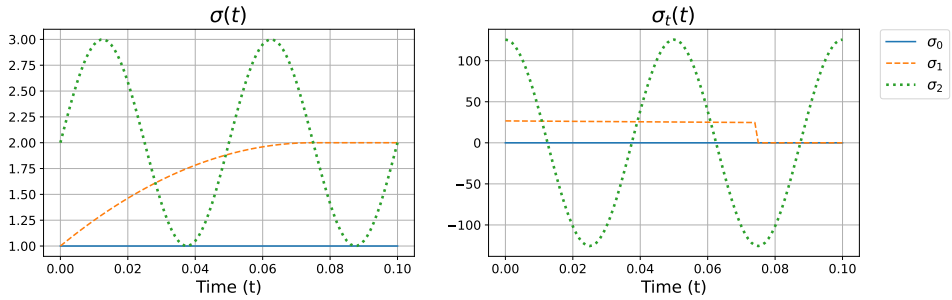


FIGURE 4. Three different choices for the time dependency of the source σ. (**Left**) Time source. (**Right**) Derivative of time source.

We employed the methodology proposed by [10] to evaluate the performance of the reconstruction formula. We assessed the feasibility of the reconstruction formula for various unknown functions $f(x)$ by using different choices of $\sigma(t)$, as depicted in Figures 5, 6 and 7. The original sources were displayed in the first column, while their projection onto the first 45 eigenvalues and the corresponding reconstructions for σ_0, σ_1, and σ_2 were shown in the second and subsequent columns. We used the projected version of the original source to compare the reconstruction of our method, as it is the best that can be obtained with a 45-frequency decomposition. We fix β depending on the source, as depicted in Table 2. Our results indicate that our proposed method achieves better accuracy than the original reconstruction method proposed by [10].

The null controls did not depend on $f(x)$ and $\sigma(t)$ and, therefore, did not require recalculation. Similarly, the coefficients $\overline{c}_k(\tau; \rho_{\tau,\beta})$ only needed to be recalculated for a fixed β value when changing the $\sigma(t)$ function, as they did not depend on $f(x)$. The observations of the solution and its time derivative in $\mathcal{O} \times (0, T)$ were perturbed (each) by a Gaussian multiplicative noise with a noise level of $100\delta\%$, more precisely, a factor $1 + \delta N(1, 0)$ where δ is the noise level (we set $\delta = 0.05$ for a 5% noise level for example) and N a Gaussian distribution of zero mean and unit standard deviation. We

observed the same robustness as claimed by [10]. This is mainly due to the fact that the reconstruction formula is unaffected by the presence of noise. To measure the accuracy of our method, we calculated the L^2 relative errors of the reconstructed source with respect to the projected source, as presented in Figures 5, 6 and 7.

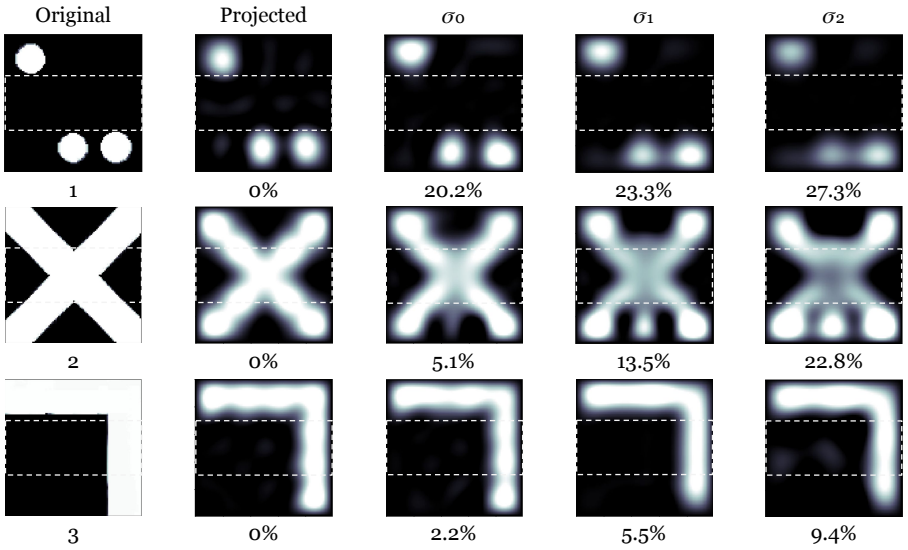


FIGURE 5. The given figure depicts the process of reconstructing various sources, represented by the function $f(x)$, where x belongs to a two-dimensional region denoted by $\Omega = (0,1)^2$. The reconstruction is done based on the local measurements taken from the observatory denoted by $\mathcal{O} = (0,1) \times (0.3, 0.7)$, which is bounded by dotted lines. The measurements are affected by normalized-Gaussian noise (with 5% of noise level). The accuracy of the reconstructions is evaluated by computing the L^2 relative error relative to the first 45 eigen-functions of the projected source. Three different cases are considered, as represented in the third, fourth, and fifth columns of the figure, where σ takes the values σ_1, σ_2, and σ_3, respectively (see Figure 4).

Table 1 shows the time consumed by each stage of our reconstruction method, displaying the total time consumed to obtain each of the experiments in Figure 5. Our reconstruction method takes on average 3.4 minutes to run, considerably better than the complexity of the original method developed by [10]. In the same computer, with the methodology of [10], for a single frequency φ_k, with $T = 0.1$ and a time step $\Delta t = 10^{-3}$, it takes approximately 18 minutes to solve the null controllability problem with relaxed minimization and in total, determining each family of controls for 45

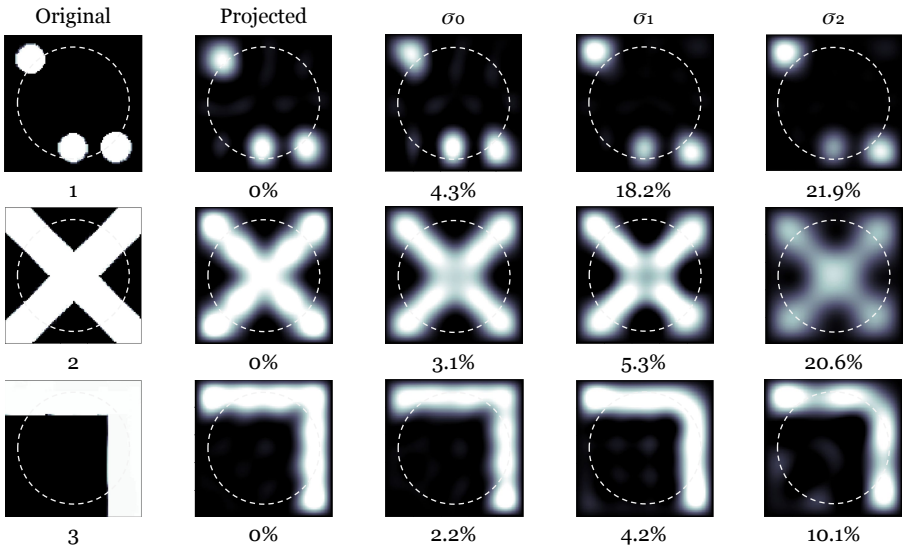


FIGURE 6. The given figure depicts the process of reconstructing various sources, represented by the function $f(x)$, where x belongs to a two-dimensional region denoted by $\Omega = (0,1)^2$. The reconstruction is done based on the local measurements taken from the observatory denoted by $\mathcal{O} = B((0.5,0.5),0.42)$, which is bounded by dotted lines. The measurements are affected by normalized-Gaussian noise (with 5% of noise level). The accuracy of the reconstructions is evaluated by computing the L^2 relative error relative to the first 45 eigen-functions of the projected source. Three different cases are considered, as represented in the third, fourth, and fifth columns of the figure, where σ takes the values σ_1, σ_2, and σ_3, respectively (see Figure 4).

frequencies takes approximately 14 hours. So there is a decrease of two orders of magnitude (250× times faster) in computational time using the proposed SOFIA basis algorithm.

Table 1 shows the aggregated dedicated complexity in the reconstruction of the coefficients as well as the total time considering the computation of the eigen-functions of the Laplacian and the pseudo-functions. We declare both times since the computation of eigen-functions is determined independently of the data of the inverse problem, and the pseudo-functions are only determined by knowing a priori the zone of observations. Meanwhile the computation of the reconstruction time complexity is broken down into three stages. The loading stage consists of retrieving the observations of both the temperature and its time derivative. The pre-computation stage consists of determining the coefficient $U_k(\tau;\beta_\tau)$ for each intermediate time τ

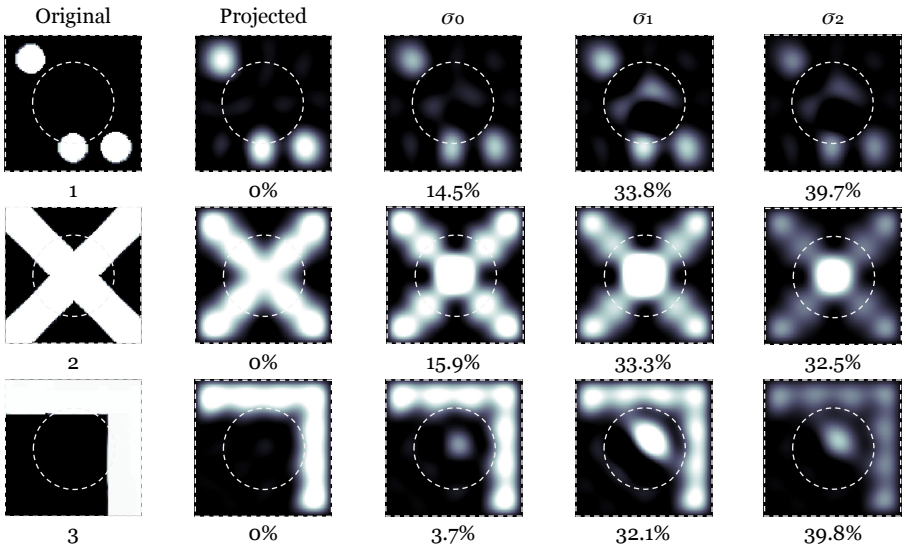


FIGURE 7. The given figure depicts the process of reconstructing various sources, represented by the function $f(x)$, where x belongs to a two-dimensional region denoted by $\Omega = (0,1)^2$. The reconstruction is done based on the local measurements taken from the observatory denoted by $\mathcal{O} = \Omega \setminus B((0.5,0.5),0.94)$, which is bounded by dotted lines. The measurements are affected by normalized-Gaussian noise (with 5% of noise level). The accuracy of the reconstructions is evaluated by computing the L^2 relative error relative to the first 45 eigen-functions of the projected source. Three different cases are considered, as represented in the third, fourth, and fifth columns of the figure, where σ takes the values σ_1, σ_2, and σ_3, respectively (see Figure 4).

at $(0,T)$ and each frequency k. While in the final stage, only the calculation of the coefficient $\overline{c}_k(\tau;\rho_{\tau,\beta})$ takes place to finish with the reconstruction of each f_k from factors a_k, C_k^1 and C_k^2.

ACKNOWLEDGEMENTS

This work was funded by ANID-Fondecyt 1201311, 1231404, CMM FB210005 Basal-ANID, FONDAP/15110009, Millennium Science Initiative Programs NCN19-161, ICN2021-004 and DO ANID Technology Center DO210001. This work was finished during the stay of A. O. at the Université Grenoble Alpes, Institut Fourier, CNRS UMR 5582.

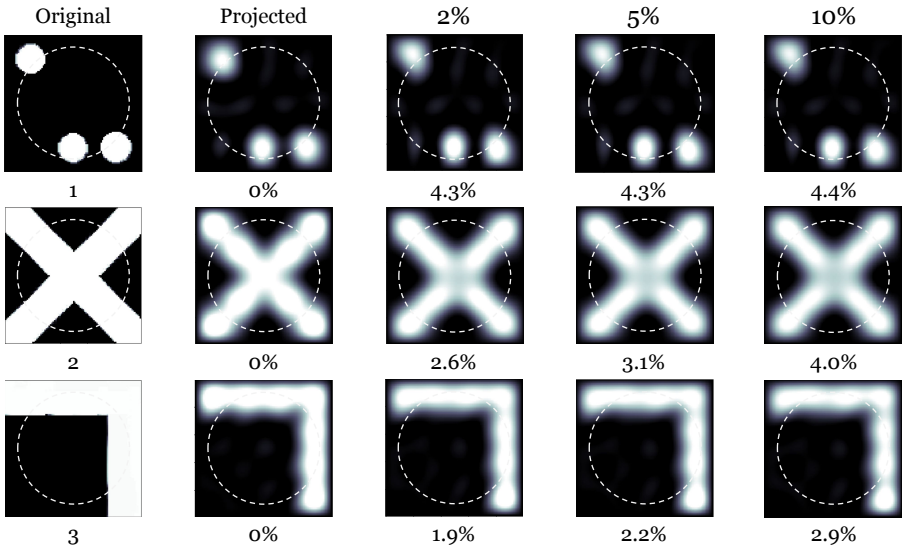


FIGURE 8. The given figure depicts the process of reconstructing various sources, represented by the function $f(x)$, where x belongs to a two-dimensional region denoted by $\Omega = (0,1)^2$. The reconstruction is done based on the local measurements taken from the observatory denoted by $\mathcal{O} = \Omega \setminus B((0.5, 0.5), 0.94)$, which is bounded by dotted lines. The measurements are affected by normalized-Gaussian noise with noise levels of 10%, 5% and 2% . The accuracy of the reconstructions is evaluated by computing the L^2 relative error relative to the first 45 eigen-functions of the projected source. In all the cases we fix the time dependency of the source in $\sigma = \sigma_1$.

REFERENCES

[1] Boulakia, M.; Grandmont, C.; Osses, A. (2009). Some inverse stability results for the bistable reactiondiffusion equation using Carleman inequalities. Comptes Rendus. Mathématique 347, 11–12, 619–622.

[2] Cannon, J.R.; DuChateau, P. (1998). Structural identification of an unknown source term in a Heat Equation. Inverse Problems 14, 535.

[3] Chavez-Silva, F. et Lebeau, G. (2016). Spectral inequality and optimal cost of controllability for the Stokes system. ESAIM: COCV 22, 1137–1162.

[4] Choulli, M; Ouhabaz, E.M.; Yamamoto, M (2006). Stable determination of a semilinear term in a parabolic equation. Communications on Pure and Applied Analysis 5(3), 447–447.

[5] Cristofol, M.; Roques, L. (2012). An inverse problem involving two coefficients in a nonlinear reactiondiffusion equation. Comptes Rendus. Mathématique 350, 9–10, 469-473.

[6] Enting, I. G., 2002: Inverse Problems in Atmospheric Constituent Transport. Cambridge University Press, 392 pp.

Reconstruction				
Load (s)	Pre (m)	Final (s)	Total (m)	**Agg** (m)
31 ± 18	1,6 ± 0,5	2,4 ± 2,1	2,2 ± 0,7	3,4 ± 0,7

Note: mean ± standard deviation, unites: seconds (s), minutes (m).

TABLE 1. The distribution of the complexity at each stage of the reconstruction and the aggregate time for all the experiments displayed in Figure 5. The above table gives the complexity in the reconstruction of the coefficients (column Total) as well as the total time considering the computation of the eigen-functions of the elliptic problem and the SOFIA basis (column Agg). The "Load" stage involves retrieving the observations of both the temperature and its time derivative. The "Pre"-computation stage determines the coefficient $U_k(\tau;\beta)$ for each intermediate time τ at $(0,T)$ and each frequency k. The "Final" stage involves the calculation of the coefficient $\overline{c}_k(\tau;\rho_{\tau,\beta})$ followed by the reconstruction of each f_k from the factors a_k, C_k^1, and C_k^2.

TABLE 2. Hyper-parameters used to obtain the results on Figure 5, 6 and 7.

	$\sigma(t)$	σ_0			σ_1			σ_2		
	$f(x)$	1	2	3	1	2	3	1	2	3
Rectangle	T	.067	.030	.042	.023	.025	.032	.065	.057	.052
	β	50	125	150	350	250	100	30	60	50
Circle	T	.050	.040	.040	.021	.063	.048	.061	.058	.052
	β	100	125	150	350	250	100	30	60	50
Complement	T	.027	.033	.033	.019	.024	.030	.028	.018	.019
of circle	β	500	125	150	350	250	200	30	60	50

TABLE 3. Hyper-parameters used to obtain the results on Figure 8.

	δ	10%			5%			2%		
	$f(x)$	1	2	3	1	2	3	1	2	3
Circle	T	.047	.040	.040	.050	.040	.040	.050	.043	.040
	β	100	125	150	100	125	150	100	125	150

[7] El Badia1, A.; Hamdi, A. (2007). Inverse source problem in an advectiondispersion-reaction system: application to water pollution. Inverse Problems, 23(5).

[8] El Badia, A. ; Ha-Duong, T. and Hamdi, A. (2005). Identification of a point source in a linear advection-dispersion-reaction equation: application to a pollution source problem. Inverse Problems 21(3), 1121–1136.

[9] Fursikov, A. V.; Imanuvilov, O. Y. (1996). Controllability of evolution equations lecture notes series 34. Research Institute of Mathematics, Global Analysis Research Center, Seoul National University.

[10] Garcia, G. C.; Osses, A.; Tapia, M. (2013). A heat source reconstruction formula from single internal measurements using a family of null controls. Journal of Inverse and Ill-posed Problems, 21(6), 755–779.
[11] García, G; Osses, A. and Puel, J.-P. (2011). A null controllability data assimilation methodology applied to a large scale ocean circulation model, M2AN 45(2), 361–386.
[12] García, G. ; Takahashi, T. (2011). Inverse problem and null-controllability for parabolic systems. J. Inv. Ill-Posed Problems 19, 379–405.
[13] Garcia, G. C.; Montoya, C. ; Osses, A. (2017). A source reconstruction algorithm for the Stokes system from incomplete velocity measurements. Inverse Problems 33, 105003.
[14] Henrquez, A.; Osses, A.; Gallardo, L. ; Diaz-Resquin, M. (2015). Analysis and optimal design of air quality monitoring networks using a variational approach. Tellus B, 67, 1–13.
[15] Hettlich1, F.; Rundell, W. (2001). Identification of a discontinuous source in the heat equation. Inverse Problems 17(5), 1465.
[16] Hmberg, D.; Lu, S.; Sakamoto, K.; Yamamoto, M. (2014). Parameter identification in non- isothermal nucleation and growth processes. Inverse Problems, 30(3).
[17] Ikehata, M. (2007). An inverse source problem for the heat equation and the enclosure method. Inverse Problems, 23, 183–202.
[18] Lebeau, G.; Robbiano, L. (1995). Contrle exact de lquation de la chaleur. Communications in Partial Differential Equations, 20(1-2), 335-356.
[19] Lebeau, G.; Jerison, L. (1999). Nodal sets of sums of eigenfunctions. Ch. 14 of Harmonic analysis and partial differential equations (Chicago, IL, 1996), p. 223, Chicago Lectures in Math. (Univ. Chicago Press, Chicago, IL, 1999).
[20] Li, J. ; Yamamoto,M. and Zou, J. (2009). Conditional stability and numerical reconstruction of initial temperature. Commun. Pure Appl. Anal. 8(1), 361–382.
[21] Ling, L. ; Yamamoto, M. ; Hon, Y.C. and Tomoya, T. (2006). Identification of source locations in two-dimensional heat equations. *Inverse Problems* 22(4), 1289–1305.
[22] Martin, P., Rosier, L., & Rouchon, P. (2014). Null controllability of the heat equation using flatness. Automatica, 50(12), 3067-3076.
[23] Mnch, A., & Zuazua, E. (2010). Numerical approximation of null controls for the heat equation: ill-posedness and remedies. Inverse problems, 26(8), 085018.
[24] Munch, A.; Pedregal, P. (2014). Numerical null controllability of the heat equation through a least squares and variational approach. European Journal of Applied Mathematics, 25(3), 277–306.
[25] Okubo, A. (1980). Diffusion and Ecological Problems: Mathematical Models, Springer, New York.
[26] Arratia, P.; Courdurier, M., Cueva, E., Osses, A. ; Palacios, B. (2021). Lipschitz Stability for Backward Heat Equation with Application to Fluorescence Microscopy. SIAM Journal on Mathematical Analysis 53(5), 5948–5978.
[27] Puel, J.-P (2009). A nonstandard approach to a data assimilation problem and Tychonov regularization revisited, SIAM J. Control Optim. 48(2), 1089–1111.
[28] Rodgers, C.D. (2000). Inverse Methods for Atmospheric Sounding: Theory and Practice. World Scientific, River Edge.
[29] Saide, P.E.; Bocquet, M. ; Osses, A. ; Gallardo, L. (2011). Constraining surface emissions of air pollutants using inverse modelling: method intercomparison and a new two-step two-scale regularization approach. Tellus B: Chemical and Physical Meteorology 63, 360–370.
[30] Yamamoto, M. (1995). Stability, reconstruction formula and regularization for an inverse source hyperbolic problem by a control method. Inverse problems, 11(2), 481.
[31] Yamatani, K.; Ohnaka, K. (1997). An estimation method for point sources of multidimensional diffusion equation. Applied Mathematical Modelling, 21(2), 77–84.